

An Eigenvalue Ratio Approach to Inferring Population Structure from Whole Genome Sequencing Data

Yuyang Xu^{1,*}, Zhonghua Liu^{1,**}, and Jianfeng Yao^{2,***}

¹Department of Statistics and Actuarial Science, The University of Hong Kong, Hong Kong SAR, China

²School of Data Science, The Chinese University of Hong Kong (Shenzhen), Shenzhen, China

**email:* xuyy@connect.hku.hk

***email:* zhhlou@hku.hk

****email:* jeff Yao@cuhk.edu.cn

SUMMARY: Inference of population structure from genetic data plays an important role in population and medical genetics studies. With the advancement and decreasing cost of sequencing technology, the increasingly available whole genome sequencing data provide much richer information about the underlying population structure. The traditional method (Patterson, Price, and Reich, 2006) originally developed for array-based genotype data for computing and selecting top principal components that capture population structure may not perform well on sequencing data for two reasons. First, the number of genetic variants p is much larger than the sample size n in sequencing data such that the sample-to-marker ratio n/p is nearly zero, violating the assumption of the Tracy–Widom test used in their method. Second, their method might not be able to handle the linkage disequilibrium well in sequencing data. To resolve those two practical issues, we propose a new method called ERStruct to determine the number of top informative principal components based on sequencing data. More specifically, we propose to use the ratio of consecutive eigenvalues as a more robust test statistic, and then we approximate its null distribution using modern random matrix theory. Both simulation studies and applications to two public data sets from the HapMap 3 and the 1000 Genomes Projects demonstrate the empirical performance of our ERStruct method.

KEY WORDS: Population structure; Principal component; Random matrix theory; Sequencing data; Spectral analysis

1. Introduction

Inference of population structure is a fundamental problem in population genetics and also plays a critical role in genetic association studies using whole genome sequencing data. For example, in population genetic studies, [Wu et al. \(2019\)](#) and [Cao et al. \(2020\)](#) performed principal component analysis (PCA) using whole genome sequencing data for the discovery of population genetic diversity in China and Singapore, respectively. In genetic association studies, the presence of population stratification may lead to spurious association estimates ([Price et al., 2006](#); [Mathieson and McVean, 2012](#); [Wang et al., 2014](#)). It is thus critical to control for the underlying population structure to avoid spurious associations when mapping the genetic basis for complex traits and human diseases

PCA-based methods have been popularized to capture the population structure from array-based genotype data ([Menozzi, Piazza, and Cavalli-Sforza, 1978](#); [Patterson, Price, and Reich, 2006](#); [Reich, Price, and Patterson, 2008](#)). These methods compute and select top principal components (PCs) that can sufficiently capture population structure ([Patterson et al., 2006](#)). Then the selected PCs can be further used to correct for population stratification bias in genetic association studies, for example, using the popular EIGENSTRAT method ([Price et al., 2006](#)).

A key question when applying PCA to genetic data is how to determine the number of PCs that can sufficiently capture the underlying unknown population structure. [Patterson et al. \(2006\)](#) modified the original Tracy–Widom (TW) test ([Tracy and Widom, 1994](#); [Johnstone, 2001](#)) and proposed the so-called sequential Tracy–Widom test using the effective (reduced) number of markers as a plug-in estimate to replace the original number of markers in the array-based genotype data set. The effective number of markers is used to estimate the number of the underlying uncorrelated markers so that the number of markers used for the Tracy–Widom test can be effectively reduced. With the use of effective number of markers,

[Patterson et al. \(2006\)](#) tried to alleviate the possible violation of the assumption in the Tracy–Widom test that the sample size and the number of genetic markers should be comparably large. We will refer to this method as the PCA-TW test throughout this paper.

However, after being applied in various empirical studies for several years, it has been found that the PCA-TW test might not perform well for capturing the true population structure in sequencing data ([Zhang, Guan, and Pan, 2012](#); [Zhang, Shen, and Pan, 2013](#); [Zhou, Marron, and Wright, 2018](#)). This is because the traditional PCA-TW test was originally developed for array-based genotype data sets that typically contain a moderate-to-high number of genetic markers, while the number of genetic markers is much larger in sequencing data. As large-scale sequencing data sets become increasingly available ([The 1000 Genomes Project Consortium, 2015](#); [Bycroft et al., 2018](#); [Wu et al., 2019](#); [Cao et al., 2020](#)), it is thus pressing to develop a new method that can resolve the following two practically important issues:

- (1) *Ultra-dimensionality* (or ultra-high-dimensionality), which refers to the scenario in which the sample-to-marker ratio n/p is nearly zero. In the random matrix theory literature, this is essentially a different regime from the one used in the PCA-TW test which assumes that n and p are comparably large ([Johnstone, 2001](#)). A genotype sequencing data set typically includes millions of markers, which makes the ratio n/p goes to an order of 10^{-4} or even smaller. In the ultra-dimensional settings, the ad hoc approach of using the effective number of markers might not perform well for sequencing data.
- (2) *Linkage disequilibrium* (LD). Genetic markers in a sequencing data set may have very high correlations (0.6–0.9). This issue becomes even worse when markers are physically close to each other on the chromosome. The theoretical validity of the PCA-TW test requires the independence assumption among the genetic markers. Hence, the presence of LD may seriously distort the null distribution of the test statistic and thus leads to biased inference. As [Patterson et al. \(2006\)](#) pointed out in their paper, there are

several issues when applying their method on data sets with large admixture-LD. To correct for the presence of LD, [Patterson et al. \(2006\)](#) recommended a modification of their PCA-TW test method using backward regression. However, this correction is computationally intensive, especially when a wide range of genetic markers are in LD with each other. Another method is LD pruning ([Purcell et al., 2007](#); [Bycroft et al., 2018](#); [Zhou et al., 2018](#); [Cao et al., 2020](#)), which removes genetic markers based on high levels of pairwise LD. This LD pruning method apparently will result in a loss of information about population structures as it might remove ancestry informative markers.

So far, several extensions of the PCA-TW test have been proposed. [Shriner \(2012\)](#) proposed an alternative plug-in estimate of the effective number of markers for the PCA-TW test. However, the reason why choosing such a plug-in estimate has not been theoretically justified. [Zhou et al. \(2018\)](#) proposed two methods to improve the PCA-TW test. The first one is the model-based method that tries to reduce the influence of the LD by correcting for the local correlation structure with an alternative eigenvalue limiting distribution. However, the simple discrete distribution of the population truth in the alternative model is chosen without theoretical justification. Their second method is to use block permutation to find out an appropriate null eigenvalue distribution. But such an approach is computationally intensive and might be computationally expensive for large-scale sequencing data.

The PCA-TW test and its extensions by [Shriner \(2012\)](#) and [Zhou et al. \(2018\)](#) all share one common key idea, that is, the sample covariance matrix can be viewed as a *finite rank perturbation* of the sample noise covariance matrix. The theory of finite-rank perturbation of a large random matrix originates from the seminal spiked population model introduced by [Johnstone \(2001\)](#). After that, there are subsequent important developments ([Paul, 2007](#); [Baik and Silverstein, 2006](#); [Baik, Arous, and P  ch  , 2005](#); [Bai and Yao, 2008](#); [Benaych-Georges and Nadakuditi, 2011](#); [Benaych-Georges, Guionnet, and Maida, 2011](#)). The theory

essentially states that the non-zero ordered eigenvalues of the sample covariance matrix \mathbf{S}_n can be separated into two parts: (1) the largest few ones are called *spikes*, whose number is the same as the number of top informative PCs minus one; (2) the remaining ones are called *bulk*, which asymptotically form a dense distribution well-separated from the spikes. Therefore, the null distribution of the top bulk eigenvalues can be used to detect spikes and to estimate the number of top informative PCs.

Unlike the PCA-TW test and its aforementioned extensions, several researchers proposed to use the ratio (or more generally, ratio-wise functions) of the consecutive eigenvalues ($\ell_1 \geq \ell_2 \geq \dots \geq \ell_n > 0$) as a more robust test statistic to detect spikes. An estimator using the ratio of eigenvalue differences $(\ell_i - \ell_{i+1})/(\ell_{i+1} - \ell_{i+2})$ as a test statistic was first proposed by [Onatski \(2009\)](#) to estimate the number of factors. Later, [Lam and Yao \(2012\)](#) and [Ahn and Horenstein \(2013\)](#) proposed an eigenvalue ratio (ER) based estimator $\operatorname{argmax}_{i \leq K_{\max}} \ell_i / \ell_{i+1}$ given a pre-determined maximum possible number of factors K_{\max} . Another type of ER-based estimator $\min\{i \geq 1 \text{ s.t. } \ell_i / \ell_{i+1} > 1 - d_T\}$ was proposed by [Li, Wang, and Yao \(2017\)](#), where d_T is chosen within $(0, 1)$. These previous results all show substantial improvements for spike detection. However, previous works on ER-based estimators focus mainly on moderate-to-high dimensional data sets with mild correlations among features. Particularly, these works still require that the sample size n and the number of features p to be of comparable magnitude. For example, the return of stocks data used in [Li et al. \(2017\)](#) has a sample-to-feature ratio of 16.89. Thus, those methods are not applicable to modern ultra-dimensional sequencing data sets where $p \gg n$, together with complicated LD structures among genetic markers.

In this paper, we propose a novel ER-based estimator to infer latent population structure (*ERStruct*) from ultra-dimensional sequencing data in the framework of analysis of variance (ANOVA) model by leveraging the fact that different latent sub-populations have differ-

ent minor allele frequencies (MAF). Although, our ER-based estimator is inspired by [Li et al. \(2017\)](#), however our method makes two new methodological contributions. First, by leveraging the recent theoretical results from random matrix theory ([Benaych-Georges and Nadakuditi, 2011](#); [Benaych-Georges et al., 2011](#); [Wang and Paul, 2014](#)), we find a new way to approximate the distribution of the eigenvalues of the sample covariance matrix under ultra-dimensionality regime by the distribution of the eigenvalues of a high-dimensional Gaussian orthogonal ensemble (GOE) matrix. Then, we use the known random matrix theory under high-dimensional regime and develop an adaptive approximation to the true null distribution, which also greatly reduces the computational burden. Second, we further resolve the LD problem in the sequencing data sets by proposing new estimates of the parameters in the approximation theory developed by [Wang and Paul \(2014\)](#) and obtain the LD-adjusted null distribution under the ultra-dimensional regime. We conduct simulation studies to compare our ERStruct method with the traditional PCA-TW method. Moreover, we apply our ERStruct method to the HapMap 3 data set ([The International HapMap 3 Consortium, 2010](#)) and the 1000 Genomes Project sequencing data set ([The 1000 Genomes Project Consortium, 2015](#)). Our proposed ERStruct method was shown to be accurate, robust and also computationally efficient.

The rest of this paper is organized as follows. In [Section 2](#), we introduce the proposed ERStruct method and its computational algorithm. In [Section 3](#), we perform simulation studies to compare our ERStruct method with the traditional PCA-TW test. In [Section 4](#), we apply our ERStruct method to two real data sets and compare its performance with the PCA-TW test. This paper ends with discussions in [Section 5](#).

2. Method

Suppose that one is interested in estimating the number of the top informative PCs (i.e., latent sub-populations) that capture population structures based on a raw n -by- p genotype

matrix \mathbf{C} which contains p genetic markers from n individuals. Each entry $\mathbf{C}(i, j) \in \{0, 1, 2\}$ represents the raw count of the minor alleles for the genetic marker j on the individual i . Assume that there are K (latent) sub-populations and the k th sub-population is of size n_k , where $\sum_{k=1}^K n_k = n$ and $1 \leq k \leq K$. To refer to a specific individual within the k th sub-population, the index of individual i is rewritten as follows:

$$i = (k, l), \quad k = 1, \dots, K \quad \text{and} \quad l = 1, \dots, n_k,$$

where l indexed the individuals within the sub-population. Using this notation, we can rewrite the raw count matrix \mathbf{C} as

$$\mathbf{C} = \left(\underbrace{\mathbf{c}_{1,1}^\top, \dots, \mathbf{c}_{1,n_1}^\top}_{\text{1st sub-pop}}, \underbrace{\mathbf{c}_{2,1}^\top, \dots, \mathbf{c}_{2,n_2}^\top}_{\text{2nd sub-pop}}, \dots, \underbrace{\mathbf{c}_{K,1}^\top, \dots, \mathbf{c}_{K,n_K}^\top}_{\text{Kth sub-pop}} \right)^\top,$$

where $\mathbf{c}_{k,l} \equiv \mathbf{C}(i, \cdot)$ is a p -dimensional vector containing the values of the genetic markers for the i th individual. We consider the following asymptotic regime throughout this paper.

ASYMPTOTIC REGIME A:

$$\begin{cases} \text{sample size } n \rightarrow \infty, \\ \text{sample-to-marker ratio } n/p \rightarrow 0. \end{cases}$$

This asymptotic regime is reasonable in whole genome sequencing data, where the number of markers p is much larger than the sample size n .

2.1 Modeling Framework

Our model builds on the key observation that individuals from different sub-populations have different minor allele frequencies (MAF) and individuals from the same sub-population have the same MAF. This observation motivates us to model the raw minor allele count data matrix using the following analysis of variance (ANOVA) model,

$$\mathbf{c}_{k,l} = \boldsymbol{\mu}_k + \boldsymbol{\varepsilon}_{k,l}, \tag{1}$$

where the p -dimensional vectors $\boldsymbol{\mu}_1, \dots, \boldsymbol{\mu}_K$ are the sub-population-specific mean counts of minor alleles across the K sub-populations, and the vectors $\boldsymbol{\varepsilon}_{1,1}, \dots, \boldsymbol{\varepsilon}_{K,n_K}$ are independent

and identically distributed noise vectors with mean zeros and covariance Σ . We emphasize here that even though we use this ANOVA model for the raw minor allele count matrix, however, our model differs from the classical ANOVA model in three ways. First, we do not know the total number of sub-populations K a priori and which individual belongs to which sub-population. Second, the sample to-marker-ratio n/p is nearly zero. Third, our model allows for the presence of different LD patterns. Those three salient features of our ANOVA model thus require modern random matrix theory to understand the sources of the variation in the sequencing data.

Following [Patterson et al. \(2006\)](#), we normalize the raw count matrix \mathbf{C} such that each column (genetic marker) has mean zero and unit variance. The estimates of the k th sub-population-specific mean vector $\hat{\boldsymbol{\mu}}_k$ and the estimate of the overall mean vector $\hat{\boldsymbol{\mu}}$ are given by

$$\begin{aligned}\hat{\boldsymbol{\mu}}_k &= \frac{1}{n_k} \sum_{l=1}^{n_k} \mathbf{c}_{k,l}, \\ \hat{\boldsymbol{\mu}} &= \frac{1}{n} \sum_{k=1}^K \sum_{l=1}^{n_k} \mathbf{c}_{k,l} = (\hat{\mu}_1, \dots, \hat{\mu}_p)^\top.\end{aligned}\tag{2}$$

We also need the following diagonal matrix with diagonal elements equal to the inverse of the standard deviations of the p genetic markers

$$\hat{\mathbf{D}} = \text{diag}\left(1/\sqrt{\hat{\mu}_j(1-\hat{\mu}_j/2)}\right), \quad 1 \leq j \leq p.$$

Then the normalized genotype data matrix is given by

$$\mathbf{M} = (\hat{\mathbf{D}} \cdot (\mathbf{c}_{1,1} - \hat{\boldsymbol{\mu}}), \dots, \hat{\mathbf{D}} \cdot (\mathbf{c}_{K,n_K} - \hat{\boldsymbol{\mu}}))^\top.\tag{3}$$

Define the sample covariance matrix of the normalized data as $\mathbf{S}_n = \mathbf{M}\mathbf{M}^\top/n$. Then, we have the standard ANOVA decomposition $\mathbf{S}_n \equiv \mathbf{S}_B + \mathbf{S}_W$, where the between-group variation \mathbf{S}_B and the within-group variation \mathbf{S}_W are given respectively by

$$\mathbf{S}_B = \sum_{k=1}^K \frac{n_k}{n} \left\{ \hat{\mathbf{D}} (\hat{\boldsymbol{\mu}} - \hat{\boldsymbol{\mu}}_k) \right\}^\top \left\{ \hat{\mathbf{D}} (\hat{\boldsymbol{\mu}} - \hat{\boldsymbol{\mu}}_k) \right\},$$

$$\mathbf{S}_W = \frac{1}{n} \sum_{k=1}^K \sum_{l=1}^{n_k} \left\{ \hat{\mathbf{D}}(\boldsymbol{\mu}_k - \hat{\boldsymbol{\mu}}_k + \boldsymbol{\varepsilon}_{k,l}) \right\}^T \left\{ \hat{\mathbf{D}}(\boldsymbol{\mu}_k - \hat{\boldsymbol{\mu}}_k + \boldsymbol{\varepsilon}_{k,l}) \right\}. \quad (4)$$

In the next section, we will perform spectral analysis for \mathbf{S}_n using modern random matrix theory.

2.2 The Spikes and the Bulk

It can be seen from Equation (4) that the within-group covariance matrix \mathbf{S}_W is essentially the noise covariance matrix. The between-group covariance matrix \mathbf{S}_B is of rank $K-1$ because it is the sum of K rank one matrices and those K between-group vectors $\{\hat{\mathbf{D}}(\hat{\boldsymbol{\mu}}_k - \hat{\boldsymbol{\mu}})\}_K$ satisfy the following linear constraint:

$$\sum_{k=1}^K \frac{n_k}{n} \hat{\mathbf{D}}(\hat{\boldsymbol{\mu}}_k - \hat{\boldsymbol{\mu}}) = \hat{\mathbf{D}} \cdot \mathbf{0} = \mathbf{0}.$$

Hence the matrix \mathbf{S}_n can be viewed as a $K-1$ rank perturbation of the sample noise covariance matrix \mathbf{S}_W . According to the finite-rank perturbation theory (Benaych-Georges and Nadakuditi, 2011; Benaych-Georges et al., 2011), under the assumption that $\min_{k \neq k^*} \|\boldsymbol{\mu}_k - \boldsymbol{\mu}_{k^*}\| \rightarrow \infty$, the non-zero ordered sample eigenvalues $\ell_1 \geq \dots \geq \ell_{n-1} > 0$ of matrix \mathbf{S}_n can be separated into two sets by relating them to the eigenvalues of either \mathbf{S}_B or \mathbf{S}_W (graphically illustrated in Figure 1):

- (1) The major part of the non-zero eigenvalues $\ell_K \geq \dots \geq \ell_{n-1} > 0$ of \mathbf{S}_n , which are infinitely many as $n \rightarrow \infty$, will converge on a closed interval $[a, b] \subseteq (0, \infty)$ to the same limiting distribution of eigenvalues of the within-group covariance matrix \mathbf{S}_W . This compact set of eigenvalues is therefore called the bulk.
- (2) The top $K-1$ eigenvalues $\ell_1 \geq \dots \geq \ell_{K-1}$ of \mathbf{S}_n will converge to certain limits $\lambda_1 \geq \dots \geq \lambda_{K-1} > b$, where b is the upper bound of the bulk. The top $K-1$ eigenvalues are called the spikes which are induced by the $K-1$ eigenvalues of the between-group covariance matrix \mathbf{S}_B .

[Figure 1 about here.]

Note that the matrix $\mathbf{S}_p = \mathbf{M}\mathbf{M}^T/p$ has the same non-zero eigenvalues as the matrix \mathbf{S}_n ,

but it is much easier to compute in practice as its dimension ($n \times n$) is much smaller than the dimension ($p \times p$) of \mathbf{S}_n . In what follows, we will use the matrix \mathbf{S}_p to compute the sample eigenvalues, and we will also infer the number of sub-populations K by performing spectral analysis on the matrix \mathbf{S}_p .

As a consequence, for any finite number m that satisfies $K \leq m \ll n$, the following results hold (almost surely) (Benaych-Georges and Nadakuditi, 2011),

$$\begin{cases} \ell_i \rightarrow \lambda_i, & 1 \leq i \leq K-1, \\ \ell_i \rightarrow b, & K \leq i \leq m. \end{cases}$$

In particular, if we let $\lambda_K = b$ and define the ratio of the sample eigenvalue limit as $\theta_i = \lambda_{i+1}/\lambda_i$, then for the sample ERs $r_i = \ell_{i+1}/\ell_i$, we have the following convergence results

$$\begin{cases} r_i \rightarrow \theta_i < 1, & 1 \leq i \leq K-1, \\ r_i \rightarrow b/b = 1, & K \leq i \leq m. \end{cases} \quad (5)$$

To avoid confusion with bulk and spike, which are typically used for eigenvalues, we will refer to the ratio r_i as the spiked ER when $1 \leq i \leq K-1$, and as the bulk ER when $K \leq i \leq n-1$ (the last ER r_n is 0 by definition).

2.3 The ER-based Estimator

Based on the above asymptotic results, theoretically we can leverage the asymptotically consistent ER-based estimator studied in Li et al. (2017) to estimate the number of latent sub-populations K as follows

$$\hat{K}'_{ER} := \min\{1 \leq i \leq n-1 \text{ s.t. } r_i > \xi_\alpha\}, \quad (6)$$

where α is the pre-specified significance level, and the critical value ξ_α is chosen as the lower α quantile of the distribution of the top bulk ER r_K (as illustrated in Figure 2).

[Figure 2 about here.]

Note that by the definition in the Equation (6), the probability of over-estimation (i.e.,

spurious detection on the bulk side) of our proposed estimator \hat{K}'_{ER} is controlled by the significance level α . However, there is no such control on the probability of under-estimation (i.e., spurious detection on the spiked side). Under-estimation might occur when the largest spiked ER $\max_{1 \leq i < K} \{r_i\}$ jumps above the critical value ξ_α , leading to an early stopping of our sequential testing procedure as given in Equation (6). Thus, in order to control the probability of under-estimation, we need to know the theoretical joint distribution of the spiked ERs. But unlike the bulk, the asymptotic distribution of the spiked eigenvalues (and thus the spiked ERs) is sensitive and varies with different distributions of the entries in the data matrix (Benaych-Georges and Nadakuditi, 2011; Benaych-Georges et al., 2011). As a result, each entry in the data matrix can substantially affect the distributions of the spikes. We observe that the last spiked ER should be asymptotically less than ξ_α , while all the bulk ERs are greater than ξ_α with a probability controlled by $1-\alpha$ as in (5). With this observation, we can control the probability of under-estimation by stopping the sequential testing procedure only if all the $(\hat{K}'_{ER} + 1)$ th to \hat{K}_c th eigenvalue ratios are confirmed to be above the critical value. Here, \hat{K}_c is some pre-specified coarse estimate \hat{K}_c for the number of sub-populations, which should be generally larger than the true K . By default, we set $\hat{K}_c = n/10$ in our algorithm to ensure $\hat{K}_c > K$ because for usual statistical estimations (and especially in the ultra-dimensional scenarios), it is crucial to have at least 10 samples in one sub-population to achieve decent estimation accuracy.

Another challenge when applying our ER-based estimator defined in Equation (6) to real data sets is to find out a proper value of ξ_α as the distribution of r_K is generally unknown. As we have mentioned in Section 1, the approach in Li et al. (2017) does not work on sequencing genotype data sets because of the severe LD and ultra-dimensionality issues. We now introduce a novel method to address these two issues and then obtain a more accurate approximation for ξ_α .

According to [Benaych-Georges et al. \(2011\)](#), the distributions of the top two bulk eigenvalues ℓ_K and ℓ_{K+1} can be approximated by the distributions of the top two eigenvalues $\tilde{\ell}_1$ and $\tilde{\ell}_2$ of the following n -by- n noise covariance matrix respectively:

$$\tilde{\mathbf{S}}_p = \frac{1}{p} \mathbf{X} \mathbf{\Sigma} \mathbf{X}^\top, \quad (7)$$

where \mathbf{X} is a n -by- p random matrix with all independent and identically distributed standard Gaussian entries. Let $\tilde{r}_1 = \tilde{\ell}_2/\tilde{\ell}_1$, the above result implies that $r_K \sim \tilde{r}_1$, where the notation \sim denotes that the two random variables on the two sides asymptotically follow the same distribution. Given the population covariance matrix $\mathbf{\Sigma}$ and a significance level α , we can in principle approximate ξ_α using the equation $P(0 < \tilde{r}_1 \leq \tilde{\xi}_\alpha) = \alpha$.

However, even if we know the true covariance $\mathbf{\Sigma}$, the top two eigenvalues $\tilde{\ell}_1$ and $\tilde{\ell}_2$ are essentially roots of a polynomial equation of order n whose distribution functions have no closed-form expressions in general. It is also computationally inefficient to use Monte Carlo method to simulate the null distribution based on the covariance matrix $\tilde{\mathbf{S}}_p$ defined in Equation (7) as we need to generate a huge n -by- p matrix \mathbf{X} multiple times, where p is at the order of millions. To solve this problem, we apply the limiting theory for the eigenvalues of the sample noise matrix developed by [Wang and Paul \(2014\)](#) under the Asymptotic Regime **A**. The theory states that the eigenvalues of $\sqrt{p/nb_p}(\tilde{\mathbf{S}}_p - a_p \mathbf{I}_n)$ converge almost surely to the *semicircle law*, where $a_p = \text{tr}(\mathbf{\Sigma})/p$ and $b_p = \text{tr}(\mathbf{\Sigma}^2)/p$ and $\text{tr}(\cdot)$ denotes the trace of a matrix. The semicircle law gives the same limiting distribution for the eigenvalues of \mathbf{W}_n/\sqrt{n} when $n \rightarrow \infty$, where \mathbf{W}_n is a n -by- n Gaussian orthogonal ensemble (GOE) matrix (i.e., a square matrix with independent entries where each diagonal entry follows $N(0, 2)$ and each off-diagonal entry follows $N(0, 1)$) ([Wigner, 1958](#); [Arnold, 1971](#)). Hence, the relationships of the top two eigenvalues of $\sqrt{p/nb_p}(\tilde{\mathbf{S}}_p - a_p \mathbf{I}_n)$ and \mathbf{W}_n/\sqrt{n} are given by

$$\sqrt{p/nb_p} \cdot (\tilde{\ell}_i - a_p) \sim w_i/\sqrt{n}, \quad i = 1, 2, \quad (8)$$

where w_1 and w_2 are the top two eigenvalues of the matrix \mathbf{W}_n . As a result, the top bulk

ER r_K can be approximated by

$$r_K \sim \tilde{r}_1 = \frac{\tilde{\ell}_2}{\tilde{\ell}_1} \sim \frac{w_2 \cdot \sqrt{\hat{b}_p/p + \hat{a}_p}}{w_1 \cdot \sqrt{\hat{b}_p/p + \hat{a}_p}} = \tilde{r}_1^*, \quad (9)$$

where

$$\hat{a}_p = \frac{1}{n-K} \sum_{i=K}^{n-1} \ell_i, \quad \hat{b}_p = \frac{p}{(n-K)^2} \sum_{i=K}^{n-1} (\ell_i - \hat{a}_p)^2, \quad (10)$$

are the two moment estimators for a_p and b_p in Equation (8) respectively.

Denote $\tilde{\xi}_\alpha^*$ as the new approximation for the critical value ξ_α in Equation (6). Given a pre-specified coarse estimator $\hat{K}_c < n-1$, our final ER-based estimator for the number of sub-populations K is

$$\hat{K}_{ER} := \min\{1 \leq i \leq \hat{K}_c \text{ s.t. } r_i, \dots, r_{\hat{K}_c} \text{ all greater than } \tilde{\xi}_\alpha^*\},$$

where we choose $\tilde{\xi}_\alpha^*$ as the lower α quantile of the distribution of \tilde{r}_1^* in Equation (9), that is,

$$P(0 < \tilde{r}_1^* \leq \tilde{\xi}_\alpha^*) = \alpha.$$

2.4 ERStruct Algorithm

We summarize our method as an algorithm to estimate K , the number of top informative PCs that capture the latent population structure, from a raw genotype data matrix \mathbf{C} below.

Algorithm ERStruct

Input: \mathbf{C} : $n \times p$ genotype data matrix

\hat{K}_c : a coarse estimate (set to $\lfloor n/10 \rfloor$ by default)

m : the number of Monte Carlo replicates

α : significance level

Output: \hat{K}_{ER} : ER estimation of the number of top informative PCs

1 $\mathbf{M} \leftarrow$ Equation (3)

2 $\mathbf{S}_p \leftarrow \frac{1}{p} \mathbf{M} \mathbf{M}^\top$

3 $\ell_1 \geq \ell_2 \geq \dots \geq \ell_{n-1} \leftarrow$ ordered non-zero eigenvalues of \mathbf{S}_p

4 $(r_1, \dots, r_{n-2}) \leftarrow (\ell_2/\ell_1, \dots, \ell_{n-1}/\ell_{n-2})$

```

5   $((w_1^{(1)} \cdots w_1^{(m)})^\top, (w_2^{(1)} \cdots w_2^{(m)})^\top) \leftarrow$  generate  $m$  replicates of the top two eigenvalues of
   GOE matrices  $\mathbf{W}_n$ 
6  for  $K \leftarrow 1$  to  $\hat{K}_c$  do
7      if no valid  $\hat{K}_{ER}$  then
8           $(\hat{a}_p, \hat{b}_p) \leftarrow$  Equations (10)
9          for  $i \leftarrow 1$  to  $m$  do
10              $(w_1, w_2) \leftarrow (w_1^{(i)}, w_2^{(i)})$ 
11              $\tilde{r}_1^{*(i)} \leftarrow$  Equation (9)
12         end for
13          $(\uparrow \tilde{r}_1^{*(1)}, \dots, \uparrow \tilde{r}_1^{*(m)}) \leftarrow$  sort  $(\tilde{r}_1^{*(1)}, \dots, \tilde{r}_1^{*(m)})$  in ascending order
14          $\tilde{\xi}_\alpha^* \leftarrow \uparrow \tilde{r}_1^{*(\lceil m\alpha \rceil)}$ 
15         if  $r_K > \tilde{\xi}_\alpha^*$  then
16              $\hat{K}_{ER} \leftarrow K$  and set  $\hat{K}_{ER}$  as valid
17         end if
18     else if  $r_K \leq \tilde{\xi}_\alpha^*$  then set  $\hat{K}_{ER}$  as not valid
19     end if
20 end for

```

3. Simulation Studies

In this section, we compare the performances of our new method ERStruct versus the original TW test (i.e., PCA-TW test without using the estimated effective number of markers; see [Patterson et al., 2006](#)) and the PCA-TW test by [Patterson et al. \(2006\)](#). The comparison is made based on how close their estimated number of PCs are to the ground truth. We consider the following two different settings.

- (1) In the uncorrelated (no LD) setting, the marker-to-marker covariance is set as $\Sigma = 0.5 \cdot \mathbf{I}_p$, and 100 independent Monte Carlo replicated samples of genotype data matrices are generated according to the ANOVA model (1). The other parameters are set so that the simulated data is similar to the 1000 Genomes Project data set with MAF less than 5% genetic markers filtered out as analyzed in Section 4. Specifically, the number of markers $p = 7,921,816$; the number of individuals $n = 2504$; the number of sub-populations $K = 26$; the numbers of individuals in each sub-population $n_k = \{96, 61, 86, 93, 99, 103, 105, 94, 99, 99, 91, 103, 113, 107, 102, 104, 99, 99, 85, 64, 85, 96, 104, 102, 107, 108\}$; the noise vector $\varepsilon_{k,l} \sim N(\mathbf{0}, 0.5 \cdot \mathbf{I}_p)$; and the mean count of minor alleles $\mu_k \sim \text{Binomial}(2, \hat{\mu}_k/2)$, with $\hat{\mu}_k$ obtained by Equation (2) in which $\mathbf{c}_{k,l}$ is the raw minor allele counts of the l th individual in the k th sub-population from the 1000 Genomes Project data set. Finally, we use a rounding mapping $x \mapsto I_{x \geq 1.5}(x) - I_{x < 0.5}(x) + 1$ so that all the simulated genotype data take values in $\{0, 1, 2\}$, where $I_A(\cdot)$ denotes an indicator function on a set A .
- (2) In the LD setting, in order to simulate local marker-to-marker correlations (the LD matrix), the noise vectors $\varepsilon_{k,l}$ within the k th sub-population are generated from the distribution $N(\mathbf{0}, 0.5 \cdot \Sigma_k)$. Each Σ_k is a block diagonal matrix extracted from the sample correlation matrix of the k th sub-population in the 1000 Genomes Project data set. All the other parameters (i.e., the number of markers p , the number of individuals n , the number of sub-populations K , the numbers of individuals in each sub-population n_k and the mean count of minor alleles μ_k) are set to be the same values as in the uncorrelated setting.

[Figure 3 about here.]

[Table 1 about here.]

The results of using the original TW-test are far from the ground truth number ($K = 26$),

as expected. With the smallest significance level $\alpha = 0.0001$ we considered, the numbers of top PCs found by the original TW test are in the range (1918, 1921) among the 100 Monte Carlo replicates in the uncorrelated setting, and it gets even worse in the LD setting where the numbers of top PCs are in the range of (2057, 2081). These simulation results show that both ultra-dimensionality and LD should be taken into account in order to accurately capture population structure in sequencing data sets.

The simulation results of using the PCA-TW test and our ERStruct method are shown in Table 1 and Figure 3. Our proposed ERStruct method outperforms the PCA-TW test. Specifically, in the uncorrelated setting which favors the PCA-TW test, our ERStruct achieve the same accuracy as the PCA-TW test. In the LD setting, 85% ($\alpha = 0.0001$) of the replicates using ERStruct are correctly estimated, and the remaining 15% of the replicates still give highly accurate estimates (ground truth $K = 26$ versus $\hat{K}_{ER} = 27$ when $\alpha = 0.0001$). In contrast, the PCA-TW test has less accurate estimates among those 100 replicates and the estimates are far away from the ground truth (ranging from 29 to 34 even when $\alpha = 0.0001$). Our ERStruct method still performs well even if the covariance matrix Σ_k varies across sub-populations.

It is worth noting that the ERStruct method is developed under the assumption that the populations share a common covariance matrix Σ while in the simulation setting with LD, we used different covariance matrices across the sub-populations. The results show that the ERStruct method is robust against this variability. One possible explanation to this robustness is that the method relies on two estimates for population spectral moments a_p and b_p given in Equation (10). It is very likely that these two estimates, derived in the case of a constant covariance matrix across all sub-populations, are still accurate for the case of different covariance matrices. However, giving a rigorous justification to this claim is difficult and out of reach from the current state of random matrix theory.

4. Real Data Analysis

In this section, we apply our proposed ERStruct to two publicly available genotype data sets to estimate the number of top informative PCs for illustration. We also include the PCA-TW method for comparison purposes.

The first data set is from the HapMap 3 project ([The International HapMap 3 Consortium, 2010](#)), which is a large-scale array-based genotype data set that includes 1115 individuals from 11 sub-populations around the world (see Web Table S1 for more detailed geographical information). Although the primary interest of this paper is focused on large-scale whole genome sequencing data, HapMap 3 includes a large number of markers (1,615,203 for the raw data in total) such that the sample-to-marker ratio of the raw data is sufficiently small ($n/p = 6.9 \times 10^{-4}$). Therefore, the HapMap 3 data set can be considered as falling into our ultra-dimensional Asymptotic Regime **A**, and can serve as a good example to illustrate our method.

The second data set is from the 1000 Genomes Project ([The 1000 Genomes Project Consortium, 2015](#)), which is a whole-genome sequencing data set with 2504 individuals from 26 sub-populations (detailed geographical information is given in Web Table S2). It was established in January 2008 with the aim to build by then the most detailed catalog of genetic variations in the human population. The 1000 Genomes Project inherits the major part of the data in HapMap 3, with additional featured sub-populations and a lot of rarer genetic variants (81,271,745 for the raw data in total) included.

Our raw data pre-processing is as follows. We first filter genetic markers using the PLINK software ([Purcell et al., 2007](#)) by imposing different levels of MAF filtering thresholds. For HapMap 3, markers with MAF less than (5%, 1%) are removed. For the 1000 Genomes Project sequencing data set, we also investigate several situations in which we remove genetic markers with MAF less than (5%, 1%, 0.5%, 0.1%, 0.05%, 0.01%). To further investigate the

performance of our ERStruct method on LD-pruned data, we performed LD-pruning on the 1000 Genomes Project data by removing genetic markers with MAF less than (5%, 1%) and LD $r^2 > 0.1$ in a window size of 10,000 base pair (bp). Then under multiple significance α levels (0.01, 0.001, 0.0001), we applied the traditional PCA-TW method and our ERStruct method to the pre-processed data sets.

[Figure 4 about here.]

[Table 2 about here.]

Since both Hapmap 3 and 1000 Genomes projects consist of human samples from known sub-populations, the number of sub-populations in each of the two data sets can be regarded as the ground truth. The estimated number of top informative PCs is expected to be close to the ground truth. As shown in Figure 4, all the ER scree plots oscillate with no specific patterns around the true r_K . This shows that the simple eyeballing method is not accurate here, and we need to estimate the number of top informative PCs using statistically more rigorous methods. More detailed estimation results are summarized in Table 2, including results on the LD-pruned 1000 Genomes Project data. Under all settings, our ERStruct gives very accurate estimates. In comparison, the PCA-TW test gives a severe over-estimation on the 1000 Genomes Project data set when the MAF filtering thresholds are 5% and 0.01%. The problem of over-estimation remains in all filtering thresholds of the smaller HapMap 3 data set, which has sample-to-marker ratios closer to the asymptotic regime assumed in the PCA-TW test ($n/p \rightarrow \text{constant} > 0$). These results are also in line with our findings in Section 3, and show that our ERStruct method is more robust to the present of LD and different MAF filtering thresholds under consideration. Even if there is a certain degree of information loss after LD pruning, our ERStruct method still performs better than the PCA-TW method.

To further assess the empirical performance of our ERStruct method, we adopt the fol-

lowing cross-validation procedure. We first randomly sampled 30% individuals from each sub-population in the original data matrix as the testing data, and the remaining 70% as the training data. We obtain the normalized data $\mathbf{M}_{\text{train}}$ and \mathbf{M}_{test} through Equation (3), respectively. Then we choose the first k PCA loadings \mathbf{V}_k computed from the normalized training data $\mathbf{M}_{\text{train}}$ and then we try to recover the normalized testing data by $\widetilde{\mathbf{M}}_k = \mathbf{V}_k \mathbf{V}_k^T \mathbf{M}_{\text{test}}$. The recovered testing data $\widetilde{\mathbf{M}}_k$ should be close to the original testing data \mathbf{M}_{test} if the top k selected PCs are sufficiently informative for capturing population structure.

We used the metric $\delta_k = \|\widetilde{\mathbf{M}}_k - \mathbf{M}_{\text{test}}\|_1$ to measure how close the recovered testing data matrix is to the original testing data matrix, where $\|\cdot\|_1$ is the induced matrix 1-norm defined as $\|\mathbf{A}\|_1 := \max_{1 \leq j \leq p} \sum_{i=1}^p |a_{ij}|$. As an example, we plot the metric δ_k versus the number of selected top PCs k using the 1000 Genomes Project data with MAF $< 5\%$ markers removed (see Web Figure S1). We found that even though the overall trend of the curve is decreasing as $k \rightarrow n$, there is clearly a local “valley” in the range (20, 50), suggesting that a good choice of top informative PCs should be in this range. We can also see from the curve that the estimated number of top informative PCs using our ERStruct method fell into this range when the significance levels are $\alpha = (0.01, 0.001, 0.0001)$, and the metric δ_k is smaller (better recovery of the testing data matrix) in comparison with the PCA-TW test.

The above real data analysis results show that our ERStruct method is more accurate and robust compared to the PCA-TW test. Based on our observations, we recommend a filtering threshold for removing genetic markers with MAF less than 1% and a significance level of 0.001, as the default parameters setting when applying our ERStruct method on whole genome sequencing data sets. In addition to this empirical recommendation, users are also suggested to perform sensitivity analysis by varying the MAF filtering threshold and significance levels.

5. Discussion

In this paper, we proposed a new method ERStruct to estimate the number of top informative PCs in whole genome sequencing data accounting for complicated LD structure between genetic markers. Our ERStruct method has been shown to outperform the traditional PCA-TW test in both simulated and real data sets. This demonstrates that our ERStruct method has wide applications to the increasingly available whole genome sequencing data sets to infer population structure (Bycroft et al., 2018; Wu et al., 2019; Cao et al., 2020).

Our ERStruct method enjoys several advantages. First, our ERStruct estimator is based on the more robust eigenvalue ratios when LD is present. Second, we obtain a more accurate adaptive null distribution approximation for the ER test statistic under the ultra-dimensional regime which is specifically developed for modern sequencing data. Third, our method is not confined to a specific LD structure among genetic markers. Even though in the real genetic data with complicated LD structures, our ERStruct can still separate the ER spikes from the ER bulk. Fourth, our ERStruct method is also computationally efficient. In fact, our ERStruct achieves almost the same computational speed as the PCA-TW test, given that $p \gg n$. For example, it took only around 30 minutes to obtain the estimate of the 1000 Genomes Project data set with MAF less than 0.05% removed (37,961,945 markers) using our ERStruct MATLAB toolbox on a server with 126G RAM and 5 cores of CPU.

Our proposed ERStruct method can also be extended to infer latent structures (like the number of latent batches) in other types of ultra-dimensional genomic data. For example, in single-cell sequencing data, most of the entries in the data matrix are zeros. Inference of latent structures in such zero-inflated sparse data matrix is still very challenging because the null distribution of the ER test statistic might be distorted (Hwang, Lee, and Schnell, 2019; Aparicio et al., 2020). More future work is needed to extend our ERStruct method for such zero-inflated data matrices.

ACKNOWLEDGEMENTS

We thank the editor, associate editor and reviewer for their valuable comments which improved this paper. Dr. Zhonghua Liu is supported by Hong Kong Research Grants Council Early Career Scheme (27307920).

DATA AVAILABILITY

The data sets used in this paper are openly available at the following links,

The International HapMap 3 Consortium (2010):

<https://www.sanger.ac.uk/resources/downloads/human/hapmap3.html>.

The 1000 Genomes Project Consortium (2015):

<https://www.internationalgenome.org/data>.

REFERENCES

- Ahn, S. C. and Horenstein, A. R. (2013). Eigenvalue ratio test for the number of factors. *Econometrica* **81**, 1203–1227.
- Aparicio, L., Bordyuh, M., Blumberg, A. J., and Rabadan, R. (2020). A random matrix theory approach to denoise single-cell data. *Patterns* **1**, 100035.
- Arnold, L. (1971). On Wigner’s semicircle law for the eigenvalues of random matrices. *Probability Theory and Related Fields* **19**, 191–198.
- Bai, Z. and Yao, J. (2008). Central limit theorems for eigenvalues in a spiked population model. *Annales de l’IHP Probabilités et Statistiques* **44**, 447–474.
- Baik, J., Arous, G. B., and Péché, S. (2005). Phase transition of the largest eigenvalue for nonnull complex sample covariance matrices. *The Annals of Probability* **33**, 1643–1697.
- Baik, J. and Silverstein, J. W. (2006). Eigenvalues of large sample covariance matrices of spiked population models. *Journal of Multivariate Analysis* **97**, 1382–1408.
- Benaych-Georges, F., Guionnet, A., and Maida, M. (2011). Fluctuations of the extreme

- eigenvalues of finite rank deformations of random matrices. *Electronic Journal of Probability* **16**, 1621–1662.
- Benaych-Georges, F. and Nadakuditi, R. R. (2011). The eigenvalues and eigenvectors of finite, low rank perturbations of large random matrices. *Advances in Mathematics* **227**, 494–521.
- Bycroft, C., Freeman, C., Petkova, D., Band, G., Elliott, L. T., Sharp, K., et al. (2018). The UK Biobank resource with deep phenotyping and genomic data. *Nature* **562**, 203–209.
- Cao, Y., Li, L., Feng, Z., Sun, X., Lu, J., Xu, Y., et al. (2020). The ChinaMAP analytics of deep whole genome sequences in 10,588 individuals. *Cell Research* **30**, 717–731.
- Hwang, J. Y., Lee, J. O., and Schnelli, K. (2019). Local law and Tracy–Widom limit for sparse sample covariance matrices. *The Annals of Applied Probability* **29**, 3006–3036.
- Johnstone, I. M. (2001). On the distribution of the largest eigenvalue in principal components analysis. *The Annals of Statistics* **29**, 295–327.
- Lam, C. and Yao, Q. (2012). Factor modeling for high-dimensional time series: Inference for the number of factors. *The Annals of Statistics* **40**, 694–726.
- Li, Z., Wang, Q., and Yao, J. (2017). Identifying the number of factors from singular values of a large sample auto-covariance matrix. *The Annals of Statistics* **45**, 257–288.
- Mathieson, I. and McVean, G. (2012). Differential confounding of rare and common variants in spatially structured populations. *Nature Genetics* **44**, 243–246.
- Menzies, P., Piazza, A., and Cavalli-Sforza, L. (1978). Synthetic maps of human gene frequencies in Europeans. *Science* **201**, 786–792.
- Onatski, A. (2009). Testing hypotheses about the number of factors in large factor models. *Econometrica* **77**, 1447–1479.
- Patterson, N., Price, A. L., and Reich, D. (2006). Population structure and eigenanalysis. *PLoS Genetics* **2**, e190.

- Paul, D. (2007). Asymptotics of sample eigenstructure for a large dimensional spiked covariance model. *Statistica Sinica* **17**, 1617–1642.
- Price, A. L., Patterson, N. J., Plenge, R. M., Weinblatt, M. E., Shadick, N. A., and Reich, D. (2006). Principal components analysis corrects for stratification in genome-wide association studies. *Nature Genetics* **38**, 904.
- Purcell, S., Neale, B., Todd-Brown, K., Thomas, L., Ferreira, M. A., Bender, D., et al. (2007). PLINK: A tool set for whole-genome association and population-based linkage analyses. *The American Journal of Human Genetics* **81**, 559–575.
- Reich, D., Price, A. L., and Patterson, N. (2008). Principal component analysis of genetic data. *Nature Genetics* **40**, 491–492.
- Shriner, D. (2012). Improved eigenanalysis of discrete subpopulations and admixture using the minimum average partial test. *Human Heredity* **73**, 73–83.
- The 1000 Genomes Project Consortium (2015). A global reference for human genetic variation. *Nature* **526**, 68–74.
- The International HapMap 3 Consortium (2010). Integrating common and rare genetic variation in diverse human populations. *Nature* **467**, 52–58.
- Tracy, C. A. and Widom, H. (1994). Level-spacing distributions and the airy kernel. *Communications in Mathematical Physics* **159**, 151–174.
- Wang, C., Zhan, X., Bragg-Gresham, J., Kang, H. M., Stambolian, D., Chew, E. Y., et al. (2014). Ancestry estimation and control of population stratification for sequence-based association studies. *Nature Genetics* **46**, 409–415.
- Wang, L. and Paul, D. (2014). Limiting spectral distribution of renormalized separable sample covariance matrices when $p/n \rightarrow 0$. *Journal of Multivariate Analysis* **126**, 25–52.
- Wigner, E. P. (1958). On the distribution of the roots of certain symmetric matrices. *Annals of Mathematics* **67**, 325–327.

- Wu, D., Dou, J., Chai, X., Bellis, C., Wilm, A., Shih, C., et al. (2019). Large-scale whole-genome sequencing of three diverse asian populations in Singapore. *Cell* **179**, 736–749.e15.
- Zhang, Y., Guan, W., and Pan, W. (2012). Adjustment for population stratification via principal components in association analysis of rare variants. *Genetic Epidemiology* **37**, 99–109.
- Zhang, Y., Shen, X., and Pan, W. (2013). Adjusting for population stratification in a fine scale with principal components and sequencing data. *Genetic Epidemiology* **37**, 787–801.
- Zhou, Y.-H., Marron, J., and Wright, F. A. (2018). Eigenvalue significance testing for genetic association. *Biometrics* **74**, 439–447.

SUPPORTING INFORMATION

Web Appendices, Tables, and Figures referenced in Section 4 are available with this paper at the Biometrics website on Wiley Online Library. A MATLAB toolbox implementing our ERStruct algorithm is available at <https://github.com/bglvly/ERStruct> including code and example data. The source code is also available at the Biometrics website on Wiley Online Library.

Received July 2021. Revised April 2022. Accepted April 2022.

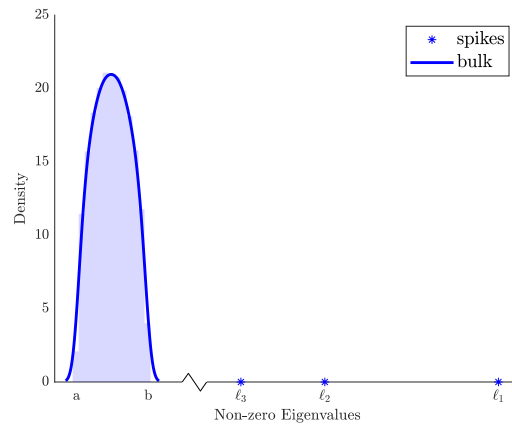


Figure 1. A typical distribution of non-zero sample eigenvalues of sample covariance matrix \mathbf{S}_n (or equivalently \mathbf{S}_p) computed from an ultra-dimensional data generated based on the uncorrelated simulation setting discussed in Section 3 (except that for a clearer view, the true number of sub-populations is chosen as $K = 4$ and the size of all the sub-populations are $n_k = \{550, 600, 650, 700\}$). The broken line in the middle of the x-axis indicates a big gap between the spikes and the bulk.

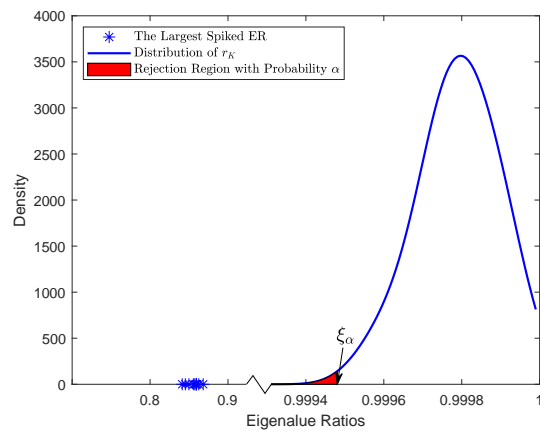


Figure 2. The largest spiked ER and the well-separated distribution of the top bulk ER r_K , generated from 100 simulations following the same setting as in Figure 1. Those ERs that are less than the critical value ξ_α will be considered as the spikes (here α is set as 0.005 for illustration).

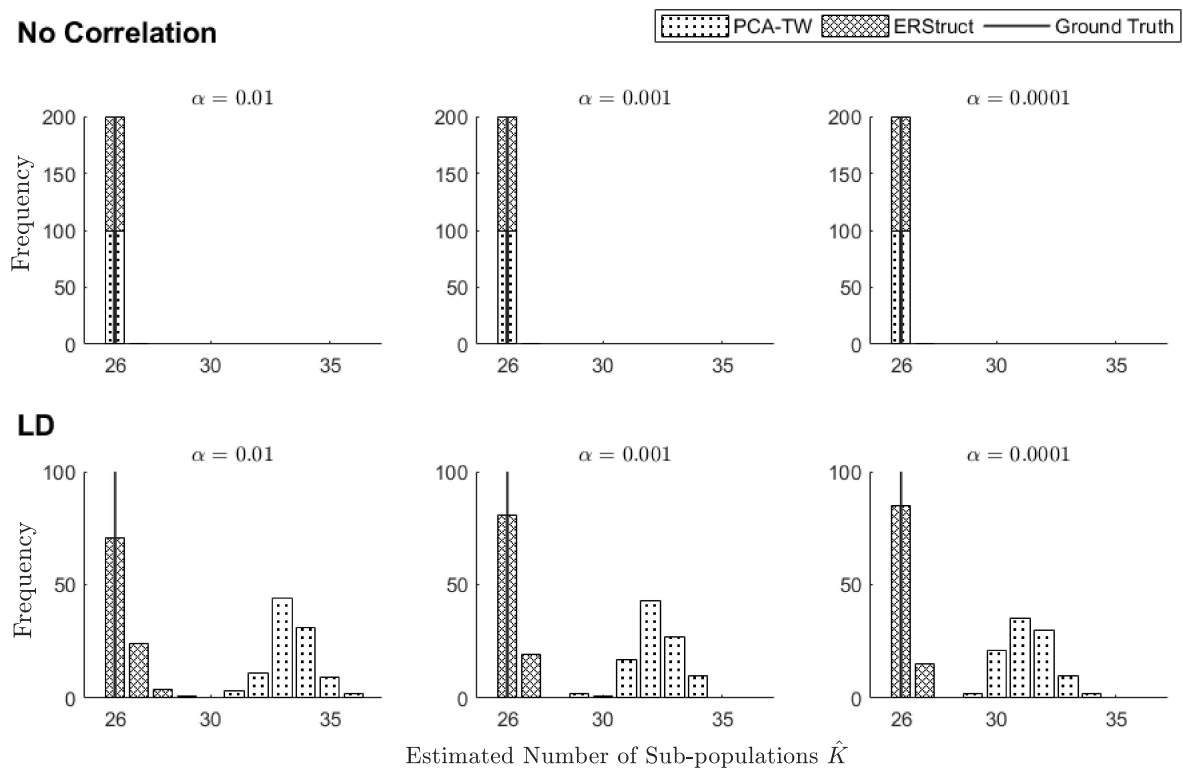


Figure 3. Histograms of the estimated number of sub-populations using the PCA-TW test (dotted) and ERStruct (crossed) in uncorrelated (upper panel) and LD settings (lower panel), each with 100 replications. The ground truth is $K = 26$.

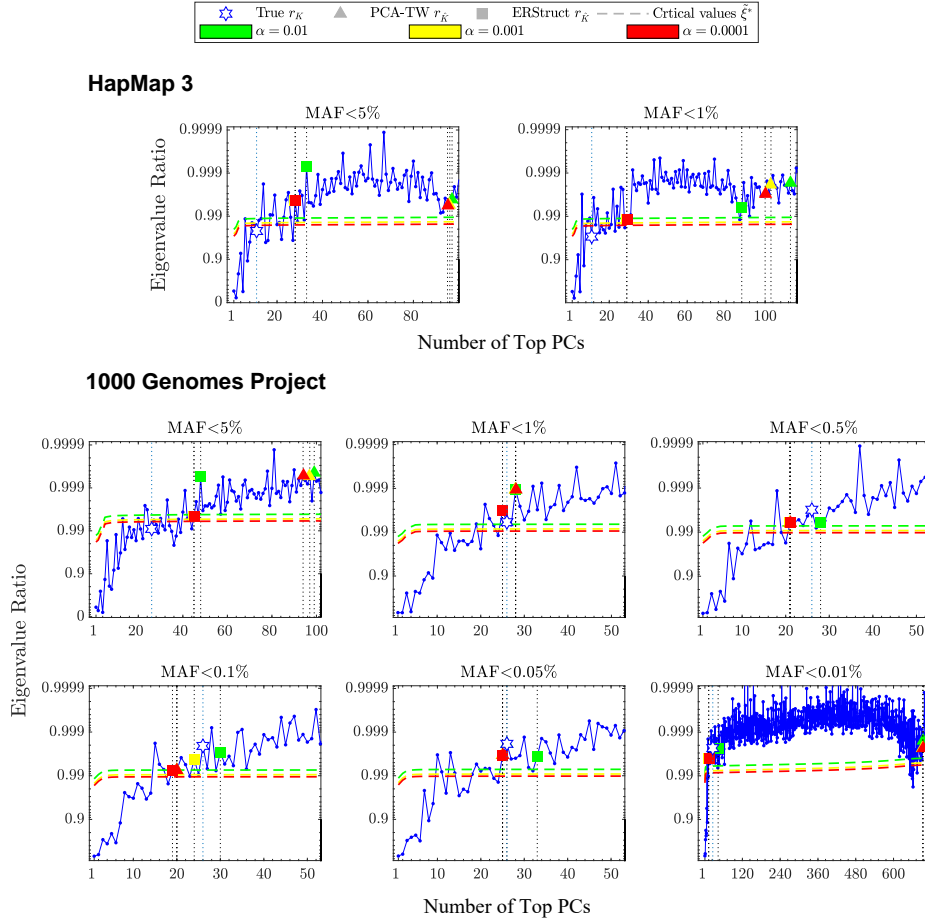


Figure 4. Scree plots of ERs computed from the HapMap 3 (11 sub-populations) and 1000 Genomes Project (26 sub-populations) data sets. Each sub-plot is created based on different MAF filtering thresholds on the raw data, in which the x-axis represents the number of top PCs, and the y-axis represents the corresponding x th top ER with a log-scale transformation $y \mapsto -\log_{10}(1-y)$ to increase visibility. True bulk ERs that correspond to the real number of sub-populations in each data set are shown in the shape of hexagram, while top bulk ERs that correspond to estimations with significance levels $\alpha = 0.01$ (red), 0.001 (yellow) and 0.0001 (green) are emphasized in the shape of triangle (PCA-TW test) and square (ERStruct). This figure appears in color in the electronic version of this article, and any mention of color refers to that version.

Table 1

Simulation results for the estimated numbers of sub-populations using the PCA-TW test and ERStruct in the LD setting. The correct estimations represent the percentages of estimations that are equal to the true number (26) of sub-populations. The range denotes the minimum and maximum estimated numbers.

α level	PCA-TW test			ERStruct		
	0.01	0.001	0.0001	0.01	0.001	0.0001
correct estimations	0	0	0	71%	81%	85%
range	[31, 36]	[29, 34]	[29, 34]	[26, 29]	[26, 27]	[26, 27]
bias	7.38	6.22	5.31	0.35	0.19	0.15
variance	0.94	1.02	1.08	0.37	0.16	0.13

Table 2

Comparison of estimations based on different filtering thresholds of the raw HapMap 3 (1,115 individuals), the raw 1000 Genomes Project (2,504 individuals), and the LD-pruned 1000 Genomes Project ($r^2 < 0.1$ in a window size 10,000 bp) data sets using the PCA-TW test and ERStruct method with significance levels $\alpha = 0.01, 0.001$ and 0.0001.

	MAF filter	no. of markers	n -to- p ratio	PCA-TW test			ERStruct		
				0.01	0.001	0.0001	0.01	0.001	0.0001
HapMap 3	MAF < 5%	1 493 644	7.5×10^{-4}	97	96	95	33	28	28
	MAF < 1%	1 601 085	7.0×10^{-4}	113	103	100	88	29	29
1000 Genomes Project (pruned)	MAF < 5%	161 842	1.5×10^{-2}	61	60	59	52	52	46
	MAF < 1%	388 636	6.4×10^{-3}	116	110	107	57	53	53
1000 Genomes Project	MAF < 5%	7 921 816	3.2×10^{-4}	99	97	94	48	45	45
	MAF < 1%	13 650 478	1.8×10^{-4}	28	28	28	28	25	25
	MAF < 0.5%	17 307 567	1.4×10^{-4}	21	21	21	28	21	21
	MAF < 0.1%	28 793 505	8.7×10^{-5}	20	20	20	24	24	19
	MAF < 0.05%	37 961 945	6.6×10^{-5}	26	25	25	33	25	25
	MAF < 0.01%	81 017 519	3.1×10^{-5}	694	693	693	43	13	13